UCRL-9529

UNIVERSITY OF CALIFORNIA

Ernest O. Lawrence Radiation Laboratory

TWO-WEEK LOAN COPY

This is a Library Circulating Copy which may be borrowed for two weeks. For a personal retention copy, call Tech. Info. Division, Ext. 5545

BERKELEY, CALIFORNIA

9529

DISCLAIMER

This document was prepared as an account of work sponsored by the United States Government. While this document is believed to contain correct information, neither the United States Government nor any agency thereof, nor the Regents of the University of California, nor any of their employees, makes any warranty, express or implied, or assumes any legal responsibility for the accuracy, completeness, or usefulness of any information, apparatus, product, or process disclosed, or represents that its use would not infringe privately owned rights. Reference herein to any specific commercial product, process, or service by its trade name, trademark, manufacturer, or otherwise, does not necessarily constitute or imply its endorsement, recommendation, or favoring by the United States Government or any agency thereof, or the Regents of the University of California. The views and opinions of authors expressed herein do not necessarily state or reflect those of the United States Government or any agency thereof or the Regents of the University of California.

UCRL-9529
Limited Distribution

UNIVERSITY OF CALIFORNIA
Lawrence Radiation Laboratory
Berkeley, California

Contract No. W-7405-eng-48

ELECTRICAL LIMITATIONS TO ENERGY RESOLUTION IN SEMICONDUCTOR PARTICLE DETECTORS

William L. Hansen and Frederick S. Goulding

April 5, 1961

ELECTRICAL LIMITATIONS TO ENERGY RESOLUTION IN SEMICONDUCTOR PARTICLE DETECTORS

William L. Hansen and Frederick S. Goulding

Lawrence Radiation Laboratory
University of California
Berkeley, California

April 5, 1961

ABSTRACT

Based on the assumption that the noise contribution of a semiconductor detector is due solely to the bulk properties of the semiconductor, equations are presented which indicate the theoretical limits of noise in detector-amplifier combinations. These equations show that an optimum amplifier time constant and detector bias voltage exist for which condition the minimum noise is independent of the semiconductor resistivity. The optimum performance of a detector-amplifier system is shown to depend only upon detector area, input capacity (less detector capacity), semiconductor minority carrier lifetime, and the transconductance of the amplifier input tube. A new detector structure including a guard-ring electrode as an integral part of the detector structure is described which largely eliminates noise due to surface leakage. Experimental results for detector leakage and energy resolution are presented which agree well with theory. The theoretical limit of noise, expressed as full width at half maximum, is in the range of 7 to 10 kev for 1-cm^2 p-type silicon detectors at 25°C.

ELECTRICAL LIMITATIONS TO ENERGY RESOLUTION IN SEMICONDUCTOR PARTICLE DETECTORS*†

William L. Hansen and Frederick S. Goulding

Lawrence Radiation Laboratory
University of California
Berkeley, California

April 5, 1961

The optimium signal-to-noise ratio obtainable from a semiconductor detector is dependent upon all of the noise generators present in the detector and the amplifier with which it is viewed. For purposes of analysis, it is convenient to treat the noise sources due to the amplifier and detector separately. Since a semiconductor junction may be looked upon as a solid ionization chamber, the general amplifier noise considerations will be the same as those developed for gaseous ionization chambers.

For noise calculations, ionization chambers may be regarded as very-high-impedance charge sources shunted by capacity. The junction detector acts in a similar way; the impedance is lower and the capacity greater than the ionization chamber, and there is a significant leakage current. The only effect of these differences is to modify the optimum design parameters of the system for the particular detector. Formulae similar to those developed for ionization-chamber amplifiers[1] are presented in Table I. In these formulae, we assume that the pulse amplifier contains single integrating and differentiating circuits having equal time constants, and that the detector collection time is very small compared with the amplifier time constant.

In Table I, note that the contribution of the tube-flicker effect to total noise is independent of the actual value of the amplifier time constant. Calculation also shows that it is small compared with the other terms in the practical case. Note that any other noise having a 1/f frequency dependence would also result in a noise component independent of the amplifier time constant.

*This work was done under the auspices of the U.S. Atomic Energy Commission.

†Presented at the International Atomic Energy Agency Conference on Nuclear Electronics, Belgrade, Yugoslavia, May 15-20, 1961.

The remaining terms in Table I all demonstrate some dependence on the amplifier time constant. The square of the tube-shot noise is inversely proportional to the amplifier time constant, while the squares of the grid-current noise, detector-leakage-current noise, and resistance noise are all linearly proportional to the amplifier time constant. Thus, there is an optimum amplifier time constant at which the signal-to-noise ratio has its greatest value.

Figure 1 presents curves calculated from Table I which illustrate the variation of mean-square noise with the various parameters in the equations. In the curves, we assume a tube grid current of 2×10^{-9} amp, a total shunt input resistance of 5 meg, and an input tube transconductance of 16 ma/v. For short amplifier time constants, tube-shot noise is dominant, whereas detector-leakage-current noise is dominant for long amplifier time constants.

Using Table I, we can calculate the optimum amplifier time constant. Since tube-shot noise and detector-leakage-current noise are dominant, the remaining terms may be neglected. Thus we have

$$\tau_{opt.} = \frac{0.35\,C}{\left(g_m i_L\right)^{1/2}} \quad . \tag{1}$$

From this result, the optimum mean square noise is then given by

$$\left\langle (\text{noise})^2 \right\rangle = 0.11\,C \left(\frac{i_L}{g_m}\right)^{1/2} \quad \text{kev}^2 \; . \tag{2}$$

This equation gives very good agreement with the curves of Fig. 1, even though it includes only the contributions due to tube-shot noise and detector-leakage-current noise.

Table II presents formulae for calculating the depletion-layer width, capacity, and diffusion and generation currents for p-type silicon at 25° C. The formulae for calculating diffusion and generation currents assume that the trap and Fermi level coincide and thus are only proportional to the real currents.[2] However, the diffusion current is very small compared to the generation current in typical detectors and therefore will be ignored.

From Eq. (2), which relates noise to detector characteristics, and the results of Table II, the mean-square noise at the optimum amplifier time constant is

$$\left\langle (\text{noise})^2 \right\rangle = \left(\frac{A}{\tau_0 g_m} \right)^{1/2} \left[0.7\, C_{in} (\rho V)^{1/4} + 2.2 \times 10^4 A (\rho V)^{-1/4} \right] \text{kev}^2, \tag{3}$$

where A is the detector area in cm^2 and C_{in} is the input capacity separate from the detector. Since the first term of Eq. (3) is proportional to $(\rho V)^{1/4}$ and the second inversely proportional, an optimum voltage must exist from a signal-to-noise point of view. This voltage is given by

$$V_{opt.} = \frac{10^9 A^2}{\rho C_{in}^2} \quad \text{volts.} \tag{4}$$

Inserting this result into Eq. (3), we have

$$\left\langle (\text{noise})^2 \right\rangle_{opt.} = 250\, A \left(\frac{C_{in}}{\tau_0 g_m} \right)^{1/2} \quad \text{kev}^2 . \tag{5}$$

When operated at the optimum time constant and voltage, Eq. (5) expresses the theoretical optimum signal-to-noise ratio for a p-type silicon detector at 25°C. For other conditions, the constant need only be modified. An important result of Eq. (5) is that ρ does not appear directly.

In order to realize practically the predicted theoretical behavior, surface effects must be eliminated. We have found that simple junction detectors have much higher leakage currents than those predicted from the equations of Table II, and that this leakage current is neither constant nor reproducible. In order to decrease surface leakage as far as possible, the guard-ring structure shown in Fig. 2 was devised. The structure was formed by etching through a photoresist mask on phosphorus-diffused p-type silicon wafers. This broke the n-type skin on the fron face into two areas--a central area used as the detector,

and a surrounding guard-ring area. The space between the guard ring and detector should be as small as practicable; it is 2 mils in the work described here.

The semiconductor guard ring resembles the conventional insulator guard ring in geometry; however, its principal roll seems to be to limit the growth of surface-inversion layers that can inject charge into the bulk material. A typical plot of detector leakage current is shown in Fig. 3 and the capacity in Fig. 4, for a 1-cm-diam detector. Both curves show the square-root law predicted by the equations of Table II. Measurements of the noise of a detector-amplifier system made by using the detector of Figs. 3 and 4 are shown in Fig. 5. The curve shown in Fig. 5 agrees very well with that predicted from Fig. 1, which indicates that the equations given in Table I accurately represent all noise sources, and that no additional significant noise source is present.

Figure 3 shows a leakage current that is poorer than average, while a better than average result is shown in Fig. 6. The lifetimes shown on Figs. 3 and 6 are calculated from the equations of Table II and serve only as a qualitative indication of the trapping levels. The interelectrode impedance for a slightly inverted surface, i.e., lightly n-type, is shown in Fig. 7. For p-type surfaces, the impedance is high at all voltages.

The main purpose here has been to evaluate electrical noise in a detector-amplifier system. It has been shown that, if surface problems are eliminated, there is reasonable agreement between theory using measured values of detector leakage and practical noise measurements. However, other limits to the particle energy resolution of practical detectors may exist.

In general, our energy-resolution experiments using β particles indicate that the limit to β-particle resolution is electrical noise. It appears that the equations derived in this paper may be used to determine the energy resolution.

We consistently achieve an energy resolution of 10 to 13 kev (full width at half maximum) using conversion electrons from a Hg^{203} source and a 1 cm-diam-detector. On the other hand, the measured

resolution figures for α particles are much larger than can be accounted for by electrical noise. The best resolution for 6-Mev α particles has been about 20 kev and, in many cases, much worse resolutions are observed. Many detectors show an auxillary upper peak; the reason for this is not clear. However, it does seem that the poor resolution of α particles is not, in general, due to unresolved multiple peaks.

A more basic understanding of the charge-collection process will be required before the ultimate in resolution of heavily ionizing particles is achieved.

FOOTNOTES

1. Gillespie, A.B., Signal, Noise, and Resolution in Nuclear Counter Amplifiers, (Permagon Press, Ltd., London, 1953).
2. Sah, C.T., Noyce, R.N., and Shockley, W., Carrier Generation and Recombination in p-n Junctions, Proc. I.R.E., 45, 1228 (1957).

Table I. Noise contributions from various sources

Noise source	Input equivalent $\langle noise \rangle^2$ (coulombs^2)	Input equivalent[a, b] $\langle noise \rangle^2$ (kev^2)	Constants
Tube-shot noise	$4\times10^{-35}\ \frac{C^2}{g_m \tau}$	$2\times10^{-2}\ \frac{C^2}{g_m \tau}$	C : total input capacity, picofarads (pf) g_m : tube mutual conductance (ma/v)
Tube flicker	$4\times10^{-37}\ C^2$	$2\times10^{-4}\ C^2$	τ : amplifier time constant (μsec)
Grid current	$3.2\times10^{-34} i_g \tau$	$1.6\times10^{-1} i_g \tau$	i_g: tube grid current (mμa)
Detector leakage	$3.2\times10^{-34} i_L \tau$	$1.6+10^{-1} i_L \tau$	i_L: detector leakage (mμa)
Input-resistance unit	$1.6+10^{-32}\ \frac{\tau}{R}$	$8\ \frac{\tau}{R}$	R: total input shunt R (CR assumed $\gg \tau$)

[a] The third column gives equivalent energy absorbed from an incident particle, assuming 3.6 ev/hole electron pair (correct for silicon).

[b] Full width at half maximum of a resolution curve is approximated by taking the square root of the sum of contributions in column 3 and multiplying by 2.3.

Table II. Detector formulae[a]

Depletion-layer width	$W = 0.32\ (\rho V)^{1/2}$ microns
Detector capacity	$C_d = 3.3 \times 10^4\ (\rho V)^{-1/2}$ pf/cm^2
Generation current	$I_g = 38\ \frac{(\rho V)^{1/2}}{\tau_0}$ mμamp/cm^2
Diffusion current	$I_d = 2.75\ \frac{\rho \cdot \ell}{\tau_0}$ mμamp/cm^2

[a] Here we define:

- W : depletion layer width,
- ρ : resistivity of bulk material (ohm-cm)
- V : applied voltage,
- C_d : detector capacity,
- I_g : generation current,
- τ_0 : minority carrier lifetime in bulk material (μsec),
- I_d : diffusion current,
- ℓ : thickness of material from which diffusion may occur (cm).

FIGURE LEGENDS

Fig. 1. Plot of noise variation vs amplifier time constant.

Fig. 2. Guard-ring detector.

Fig. 3. Typical relationship of leakage current to voltage.

Fig. 4. Typical relationship of voltage to capacity.

Fig. 5. Typical plot of noise variation vs amplifier time constant.

Fig. 6. Curve showing less than average leakage current.

Fig. 7. Interelectrode impedance characteristic (n-type surface).

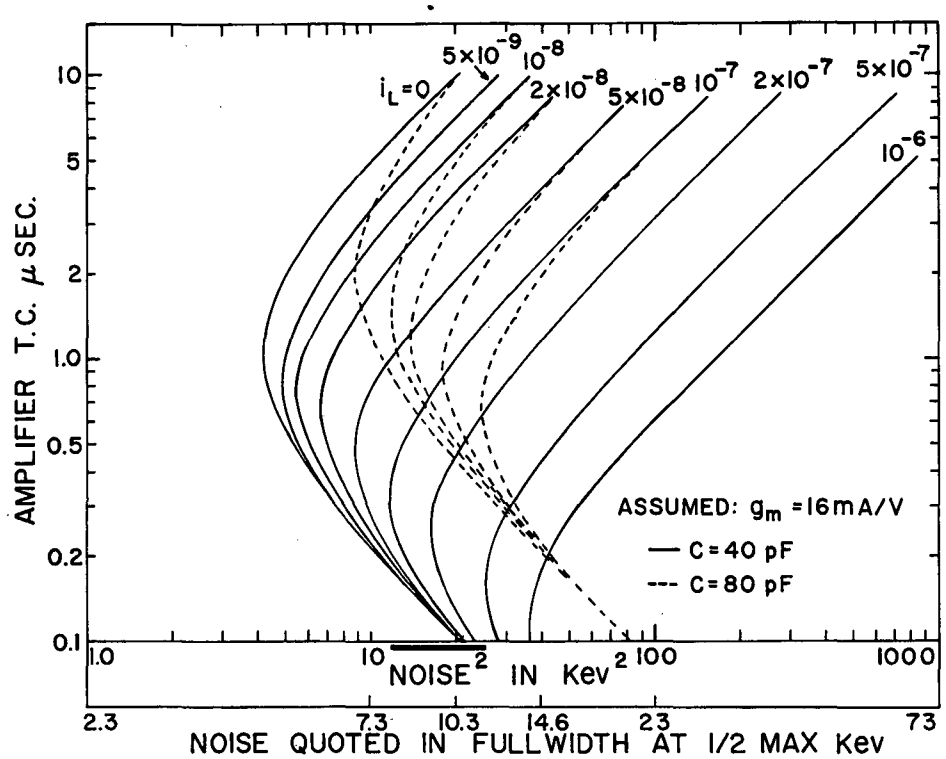

MU-21766

Fig. 1

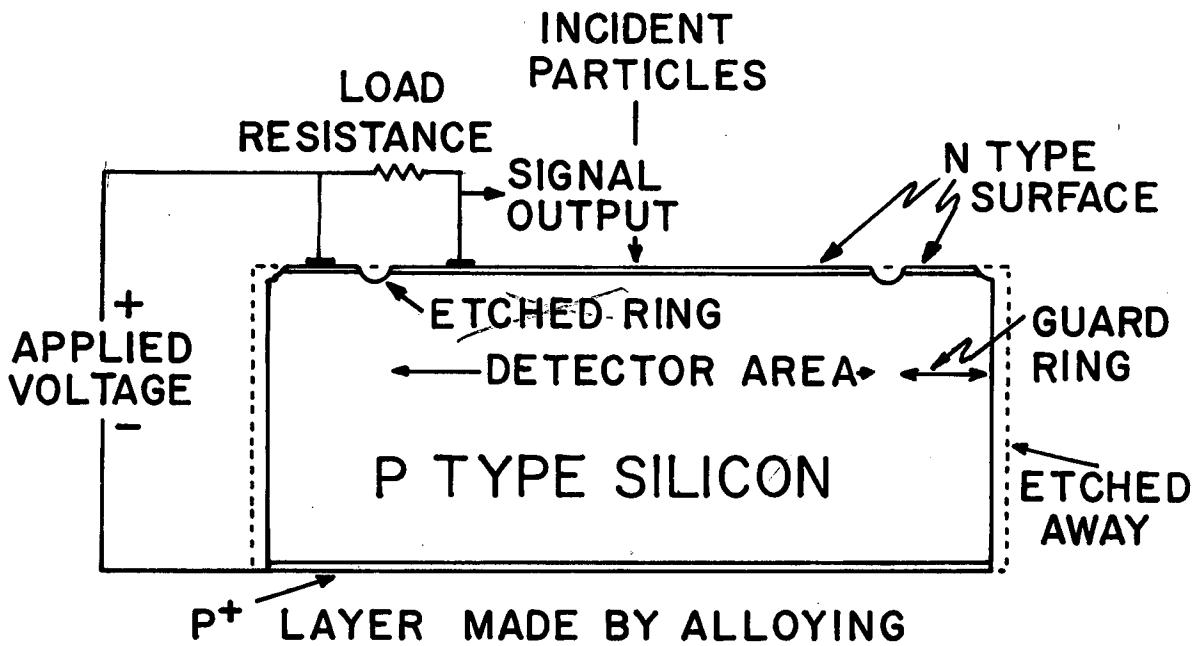

MU-21767

Fig. 2

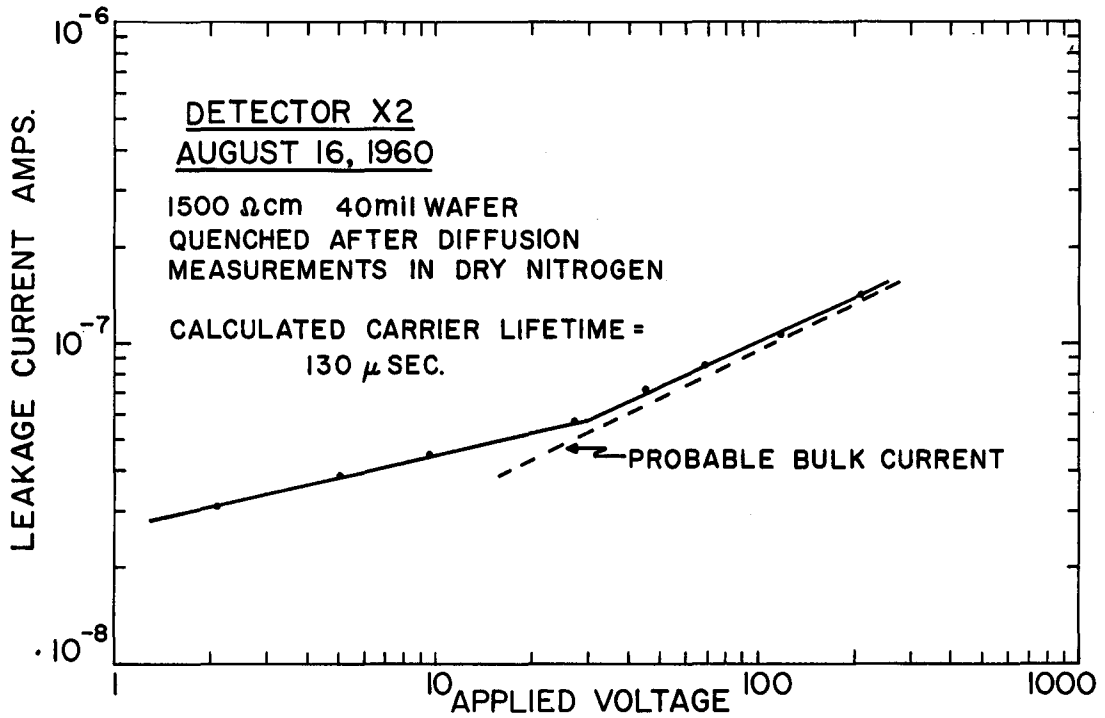

MU-21770

Fig. 3

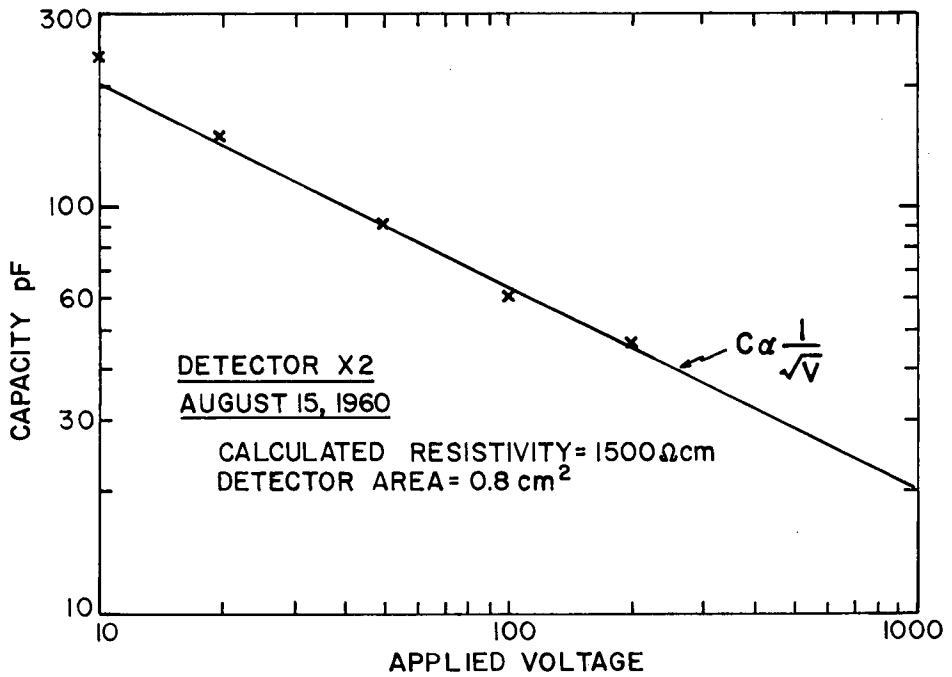

MU-21769

Fig. 4

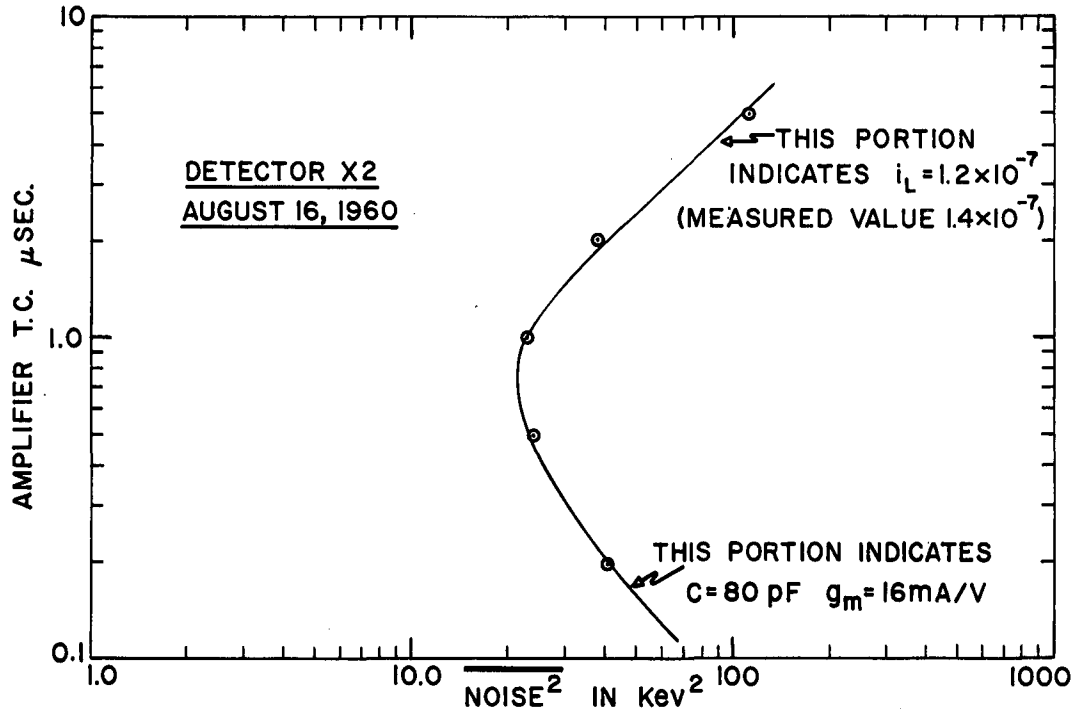
DETECTOR X2
AUGUST 16, 1960
THIS PORTION INDICATES $i_L = 1.2 \times 10^{-7}$ (MEASURED VALUE 1.4×10^{-7})
THIS PORTION INDICATES C = 80 pF g_m = 16mA/V
AMPLIFIER T.C. μSEC.
10
1.0
0.1
1.0
10.0
100
1000
$\overline{\text{NOISE}^2}$ IN Kev^2

MU-21771

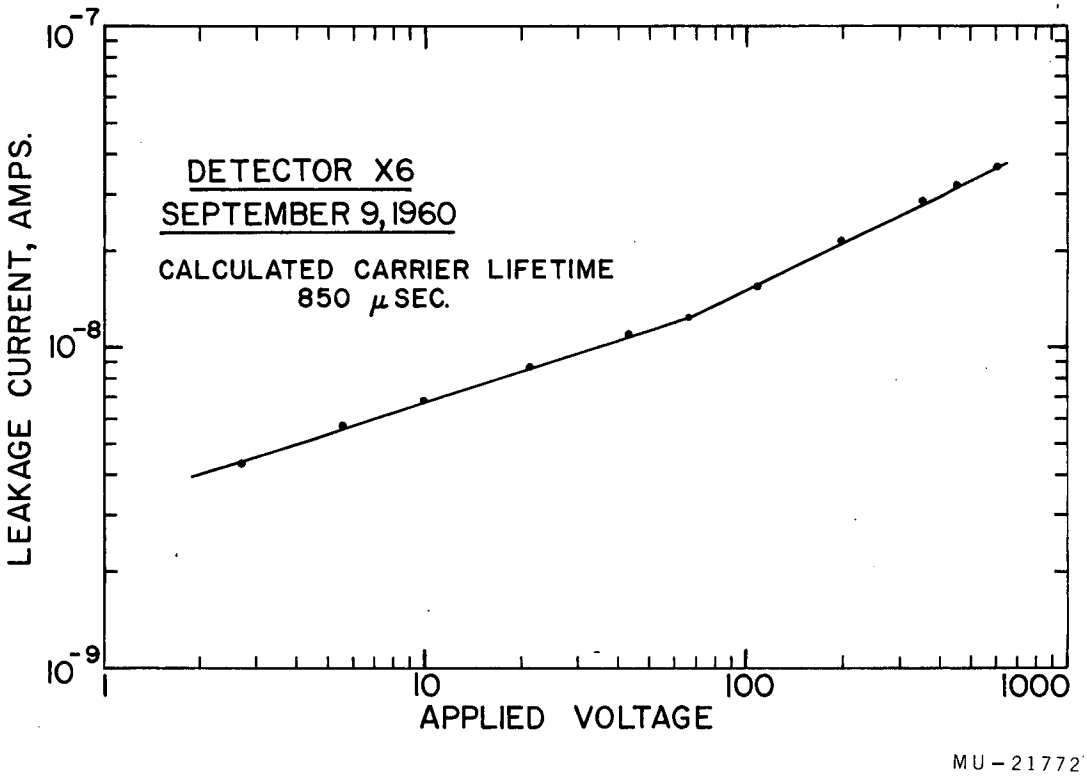
DETECTOR X6
SEPTEMBER 9, 1960
CALCULATED CARRIER LIFETIME
850 μSEC.
LEAKAGE CURRENT, AMPS.
10^-7
10^-8
10^-9
1
10
100
1000
APPLIED VOLTAGE
MU-21772

Fig. 6

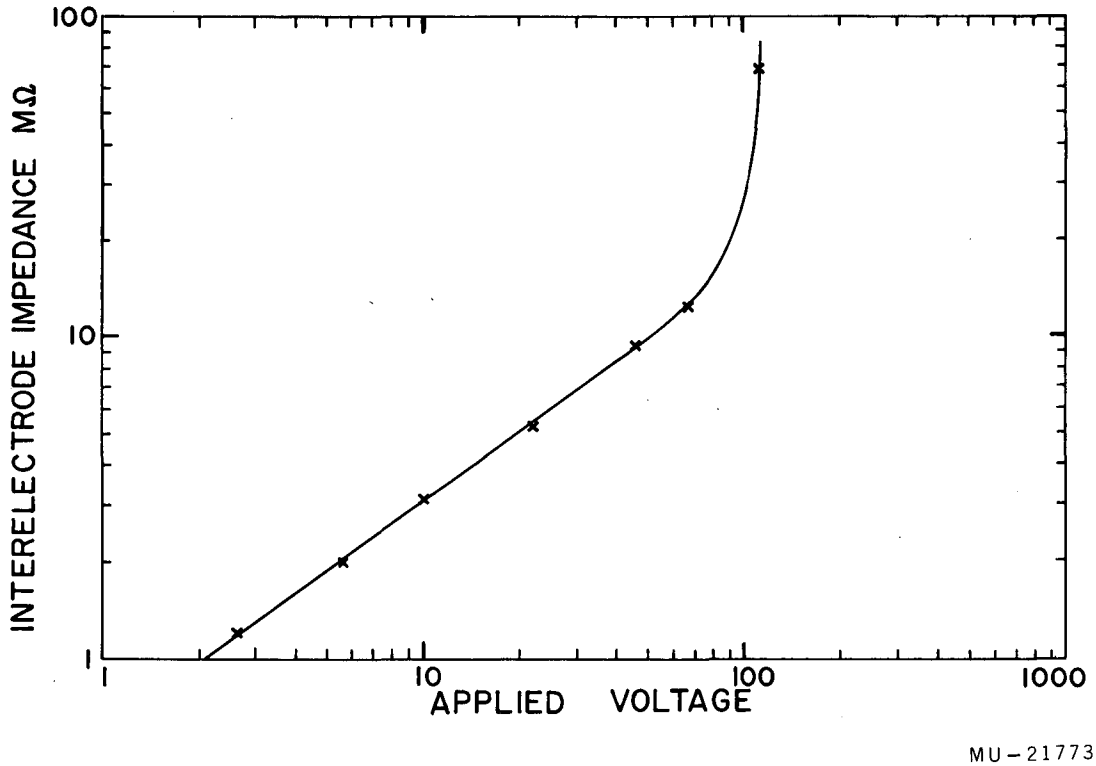
100
10
1
INTERELECTRODE IMPEDANCE MΩ
1
10
100
1000
APPLIED VOLTAGE
MU-21773

Fig. 7

This report was prepared as an account of Government sponsored work. Neither the United States, nor the Commission, nor any person acting on behalf of the Commission:

A. Makes any warranty or representation, expressed or implied, with respect to the accuracy, completeness, or usefulness of the information contained in this report, or that the use of any information, apparatus, method, or process disclosed in this report may not infringe privately owned rights; or

B. Assumes any liabilities with respect to the use of, or for damages resulting from the use of any information, apparatus, method, or process disclosed in this report.

As used in the above, "person acting on behalf of the Commission" includes any employee or contractor of the Commission, or employee of such contractor, to the extent that such employee or contractor of the Commission, or employee of such contractor prepares, disseminates, or provides access to, any information pursuant to his employment or contract with the Commission, or his employment with such contractor.